J Physiol 590.7 (2012) pp 1737–1755

The Journal of Physiology

Excitatory inputs to four types of spinocerebellar tract neurons in the cat and the rat thoraco-lumbar spinal cord

Sony Shakya Shrestha[1], B. Anne Bannatyne[1], Elzbieta Jankowska[2], Ingela Hammar[2], Elin Nilsson[2] and David J. Maxwell[1]

[1]*Spinal Cord Group, Institute of Neuroscience and Psychology, College of Medicine, Veterinary Medicine and Life Sciences, University of Glasgow, Glasgow G12 8QQ, UK*

[2]*Department of Physiology, Sahlgrenska Academy, University of Gothenburg, 405 30 Göteborg, Sweden*

Key points

- For co-ordinated limb movements, the brain needs to be provided with continuous feedback information from the spinal cord.
- We investigated the types of information forwarded to the cerebellum by four populations of neurons.
- Cells were classified according to their electrophysiological properties in cats and location within the grey matter in rats.
- We used immunochemistry to identify excitatory (glutamatergic) terminals and to differentiate between terminals of peripheral sensory fibres and terminals of spinal or supraspinal neurons in contact with labelled cells.
- Our results revealed marked differences between these four populations.
- These findings improve our understanding of the functional connectivity between the spinal cord and the cerebellum and provide new insights into the role of the cerebellum in controlling limb movements.

Abstract The cerebellum receives information from the hindlimbs through several populations of spinocerebellar tract neurons. Although the role of these neurons has been established in electrophysiological experiments, the relative contribution of afferent fibres and central neurons to their excitatory input has only been estimated approximately so far. Taking advantage of differences in the immunohistochemistry of glutamatergic terminals of peripheral afferents and of central neurons (with vesicular glutamate transporters VGLUT1 or VGLUT2, respectively), we compared sources of excitatory input to four populations of spinocerebellar neurons in the thoraco-lumbar spinal cord: dorsal spinocerebellar tract neurons located in Clarke's column (ccDSCT) and in the dorsal horn (dhDSCT) and ventral spinocerebellar tract (VSCT) neurons including spinal border (SB) neurons. This was done on 22 electrophysiologically identified intracellularly labelled neurons in cats and on 80 neurons labelled by retrograde transport of cholera toxin b subunit injected into the cerebellum of rats. In both species distribution of antibodies against VGLUT1 and VGLUT2 on SB neurons (which have dominating inhibitory input from limb muscles), revealed very few VGLUT1 contacts and remarkably high numbers of VGLUT2 contacts. In VSCT neurons with excitatory afferent input, the number of VGLUT1 contacts was relatively high although VGLUT2 contacts likewise dominated, while the proportions of VGLUT1 and VGLUT2 immunoreactive terminals were the reverse on the two populations of DSCT neurons. These findings provide morphological evidence that SB neurons principally

DOI: 10.1113/jphysiol.2011.226852

receive excitatory inputs from central neurons and provide the cerebellum with information regarding central neuronal activity.

(Received 20 December 2011; accepted after revision 21 February 2012; first published online 27 February 2012)
Corresponding author D. J. Maxwell: Spinal Cord Group, Institute of Neuroscience and Psychology, College of Medicine, Veterinary Medicine and Life Sciences, University of Glasgow, Glasgow G12 8QQ, UK.
Email: david.maxwell@glasgow.ac.uk

Abbreviations ABSM, anterior biceps and semimembranosus; ANOVA, analysis of variance test; 4-AP, 4-aminopyridine; cc, Clarke's column; CTb, cholera toxin b subunit; DAB, 3,3′-diaminobenzidine; dh, dorsal horn; DSCT, dorsal spinocerebellar tract; EPSP, excitatory post-synaptic potential; FDL, flexor digitorum and hallucis longus; GS, gastrocnemius–soleus; HRP, horseradish peroxidise; IgG, immunoglobulin gamma; IPSP, inhibitory post-synaptic potential; L, lumbar; MLF, medial longitudinal fascicle; PB, phosphate buffer; PBS, phosphate-buffered saline; PBST, phosphate-buffer saline containing 0.3% trition; PBSt, posterior biceps and semitendinosus; PL, plantaris; PSP, post-synaptic potential; Q, quadriceps; Sart, sartorius; SB, spinal border; SP, superficial peroneal; Th, thoracic; VGLUT, vesicular glutamate transporter; VSCT, ventral spinocerebellar tract.

Introduction

A first step towards understanding the role of the cerebellum in the control of movements is to determine the nature of the information forwarded to it. Electrophysiological studies of input to the four main populations of lumbar spinocerebellar neurons have revealed considerable differences between them. Dorsal spinocerebellar tract (DSCT) neurons were primarily found to carry information about peripheral events, subpopulations of these neurons monitoring input from different types of receptors including muscle spindles, Golgi tendon organs, joint and cutaneous receptors (for a review see Oscarsson, 1965; Edgley & Jankowska, 1988). However, even though input to individual DSCT neurons is drawn from fairly restricted receptive fields, information carried by the whole population of these neurons has been found to reflect whole limb kinematics (Bosco & Poppele, 2001). Direct input to ventral spinocerebellar tract (VSCT) neurons likewise originates from several categories of afferents, but input to individual neurons is drawn, as a rule, from several muscles (for reviews see Oscarsson, 1965; Burke *et al.* 1971; Lundberg & Weight, 1971). In addition, VSCT neurons monitor activity of spinal interneuronal networks (Lundberg, 1971) and descending commands to a much greater extent (see Hammar *et al.* 2011). For instance, DSCT neurons in Clarke's column were found to receive direct excitatory input from corticospinal tract neurons (Hantman & Jessell, 2010) but only indirect excitatory input from reticulospinal neurons (Hammar *et al.* 2011), while VSCT neurons are excited both directly and indirectly by reticulospinal, vestibulospinal, corticospinal and rubrospinal neurons (Baldissera & Roberts, 1976; Hammar *et al.* 2011; Jankowska *et al.* 2011). However, in electrophysiological experiments the relative contribution of afferent fibres and central neurons to the input of subpopulations of VSCT and DSCT neurons could only be estimated approximately. For instance, even if a high proportion of the spinal border (SB) subpopulation of VSCT neurons appeared to be primarily inhibited following stimulation of hindlimb muscle nerves (Burke *et al.* 1971; Lundberg & Weight, 1971), it could not be excluded that low threshold afferents from other parts of the body and/or slower conducting high-threshold muscle or skin afferents evoked synaptic actions nor that those coinciding with inhibitory post-synaptic potentials (IPSPs) evoked by faster conducting lower threshold afferents remained undetected. Conversely, as input from only some descending tract neurons to DSCT neurons has been investigated so far, it could not be excluded that other descending neurons or intraspinal neurons provided major input to them. The main aim of the present study was therefore to compare the relative contribution of primary afferents and central neurons to excitatory synaptic input to two populations of DSCT and two populations of VSCT neurons: (1) DSCT neurons located in Clarke's column with their main input from group Ia afferents (ccDSCT neurons); (2) DSCT neurons located in the dorsal horn with input from group II afferents and skin afferents but not group I afferents (dhDSCT neurons; Edgley & Jankowska, 1987); (3) VSCT neurons located in the medial part of lamina VII, with excitatory peripheral input mainly from group Ib afferents (Ib-VSCT neurons; which will be referred to as VSCT neurons); and (4) VSCT neurons located at the border between the white and grey matter in the ventral horn, with excitatory peripheral input mainly from group Ia afferents, or apparently devoid of such input (which will be referred to as spinal border, SB, neurons). SB neurons with negligible input from primary afferents have been of particular interest because of recent indications that their main function might be different from those of other spinocerebellar neurons; to forward information not so much about input to spinal neurons as about the probability of activation of motoneurons by descending commands (see Hammar *et al.* 2011; Jankowska *et al.* 2011).

In the first series of experiments in cats, spinocerebellar tract neurons were initially identified and characterized electrophysiologically. Representative neurons of the four populations were then injected with a mixture of rhodamine-dextran and Neurobiotin. In the second series of experiments, we took advantage of the fact that the organization of the various subpopulations of spinocerebellar tract neurons, in terms of location and axonal projections, is the same in the cat and rat (Matsushita & Hosoya, 1979; Matsushita *et al.* 1979). The features of neurons analysed in the cat could thus be compared to features of corresponding rat neurons identified according to their anatomical location by retrograde transport of the b-subunit of cholera toxin (CTb), injected into the cerebellum. In both species, glutamatergic nerve terminals in contact with labelled neurons were analysed immunohistochemically. In order to differentiate between terminals of different origin we used antibodies against vesicular glutamate transporter 1 (VGLUT1) to label primary afferent terminals (Varoqui *et al.* 2002; Todd *et al.* 2003; Alvarez *et al.* 2004) and against vesicular glutamate transporter 2 (VGLUT2) to mark axon terminals of spinal interneurons and most descending tract neurons with the exception of the corticospinal tracts (A. Du Beau, S. Shakya Shrestha & D. J.Maxwell, in preparation). As shown previously the distribution of VGLUT1 and VGLUT2 terminals in cat spinal cord grey matter is very similar to that in rat spinal cord, although the patterns of the expression of these two markers were originally investigated in rat spinal cord only (Varoqui *et al.* 2002; Todd *et al.* 2003). Furthermore, all cat excitatory interneurons studied previously expressed VGLUT2 but never VGLUT1 (Bannatyne *et al.* 2009).

Methods

Ethical approval

The study was carried out on a sample of 22 neurons labelled in 6 adult cats (2–5 cells from each animal) and on 80 neurons labelled in four adult Sprague–Dawley rats (Harlan, Bicester, UK). Cats (2.5–3.8 kg) were bred and housed under veterinary supervision at the Laboratory of Experimental Biomedicine at Sahlgrenska Academy where the electrophysiological experiments were carried out. All experimental procedures were approved by the Ethics Committee for Animal Research at the University of Gothenburg (Göteborgs Djurförsöksetiska Nämnd). Experiments on rats were conducted according to British Home Office legislation and were approved by the University of Glasgow Ethics committee. All comply with National Institute of Health and European Union guidelines for animal care and with the ethical policies and regulations of The Journal of Physiology (Drummond *et al.* 2010).

Experimental procedures on cats

Surgical procedures. General anaesthesia was induced with sodium pentobarbital (Apoteksbolaget, Sweden; 40–44 mg kg^{-1} I.P.) and maintained with intermittent doses of α-chloralose (Rhône-Poulenc Santé, France; 5 mg kg^{-1} I.V., administered every 1–2 h up to 30 mg kg^{-1} and every 2–3 h up to 55 mg kg^{-1} thereafter). Additional doses of α-chloralose were given when motor reactions were evoked during dissection and when increases in the continuously monitored blood pressure or heart rate were evoked by any experimental procedures. Atropine (0.05–0.2 mg kg^{-1} I.M.) was sometimes administered during the preliminary surgical procedures to reduce tracheal secretion. During recordings, neuromuscular transmission was blocked by using pancuronium bromide (Pavulon, Organon, Sweden; about 0.2 mg kg^{-1} h^{-1} I.V.) and the animals were artificially ventilated. The effectiveness of synaptic transmission was increased by intravenous administration of 4-aminopyridine (4-AP, Sigma, USA; 0.1–0.2 mg kg^{-1}). Mean blood pressure was maintained at 100–140 mmHg and the end-tidal concentration of CO_2 at about 4% by adjusting the parameters of artificial ventilation and the rate of a continuous infusion of a bicarbonate buffer solution with 5% glucose (1–2 ml h^{-1} kg^{-1}). Core body temperature was kept at about 38°C by servo-controlled infrared lamps.

Laminectomy was performed to expose the spinal cord from the third to the sixth lumbar (L3–L6) segments and at the level of the low thoracic (Th10–Th12) segments. The dura mater remained intact except for small holes (about 1 mm^2) over the dorsal columns through which recording electrodes were inserted. The caudal part of the cerebellum was exposed to allow insertion of tungsten electrodes (30–200 kΩ) used to stimulate axons of spinocerebellar neurons to activate them antidromically and to stimulate reticulospinal axons running in the medial longitudinal fascicle (MLF).

Cerebellar stimulation sites were located ipsilateral to DSCT and contralateral to VSCT and SB neurons, just rostral to or within the nucleus interpositus (at Horsley–Clarke coordinates about P 7, L 3.0–3.5, H 0 to –1). They were marked by electrolytic lesions made at the end of experiments and reconstructed histologically. Axons within the MLF were stimulated ipsilateral with respect to the location of the neurons recorded from. The stimuli were applied at Horsley–Clarke coordinates P 7–9, L 0.5–0.8, H about –5. The final electrode position was adjusted while recording descending volleys from the surface of the spinal cord at the Th11–Th12 level. The electrodes were left at locations from which distinct descending volleys were evoked at thresholds of 10–20 μA; they were near maximal at 50–100 μA for cerebellar stimulation sites and at 100–150 μA for MLF stimulation sites.

In order to identify peripheral inputs, several left hindlimb nerves were dissected free, transected and mounted on stimulating electrodes. They included: quadriceps (Q) and sartorius (Sart) branches of the femoral nerve mounted in subcutaneous cuff electrodes; the posterior biceps and semitendinosus (PBSt), anterior biceps and semimembranosus (ABSM), sural (Sur), superficial peroneal (SP), gastrocnemius–soleus (GS), plantaris (PL) and/or flexor digitorum and hallucis longus (FDL) branches of the sciatic nerve mounted on pairs of silver electrodes in a paraffin oil pool.

Stimulation. Peripheral nerves were stimulated with constant voltage stimuli at intensities expressed in multiples of threshold (T) for the activation of the most excitable fibres. Afferent volleys following these stimuli (recorded from the cord dorsum at the L5 segmental level) were used to determine the central latencies of postsynaptic potentials (PSPs). Intracerebellar axonal branches of spinocerebellar neurons were stimulated by using 0.2 ms long constant current pulses at intensities $\leq$100 μA. Axons of these neurons within the ipsilateral or contralateral funiculus at the Th11–Th12 level were stimulated extradurally, with two silver ball electrodes in contact with its surface, using constant current pulses of 100–500 μA.

Criteria for identification of different populations of spinocerebellar neurons and labelling. DSCT neurons were searched for in the L3–L4 segments. ccDSCT neurons were found at the medial border of the dorsal horn at depths of 2–2.5 mm from the surface of the dorsal columns at which large field potentials were evoked from group I muscle afferents at thresholds $<$2T and latencies of $\leq$1 ms. dhDSCT neurons were found more laterally and more superficially, at 1.2–1.8 mm from the surface of the dorsal columns and often caudal to Clarke's column. In this area, large synaptic field potentials were evoked by group II, but not group I muscle afferents (Edgley & Jankowska, 1987). In addition, dhDSCT neurons had a characteristic input from group II muscle afferents and cutaneous afferents (Edgley & Jankowska, 1988): from muscle nerves at 3–5T and latencies of 2–3 ms and from cutaneous afferents at minimal latencies of 1–2 ms.

VSCT neurons were searched for in the L4 and L5 segments. The SB subpopulation of these neurons was identified by their location within a 100–200 μm wide strip at the border between the lateral funiculus and the ventral horn (usually at depths 1.8–2.2 mm from the surface of the lateral funiculus at an angle of 10–20 deg from vertical) and by their monosynaptic input from reticulospinal neurons (MLF; Hammar *et al.* 2011) and inhibitory input from group I and high-threshold muscle afferents (Burke *et al.* 1971; Lundberg & Weight, 1971). When present, excitatory input from primary afferents was evoked from group Ia afferents, but preference was given to SB neurons with exclusively inhibitory input from peripheral nerves (see the last section of the Introduction). More medially distributed VSCT neurons were identified by their location at depths 2.4–3.9 mm from the surface of the dorsal columns (at an angle of about 0 deg), at which focal field potentials were evoked from both group I and II, or only group II muscle afferents (Hammar *et al.* 2002), and by their characteristic input properties: excitatory from group Ib afferents and inhibitory from group I and high-threshold muscle afferents (Eccles *et al.* 1961*a*). Representative examples of PSPs from each of these four neuronal populations are shown in Fig. 1.

Once the neurons were identified, they were labelled intracellularly by ionophoresis with a mixture of equal proportions of 5% tetramethylrhodamine-dextran (Molecular Probes, Inc., Eugene, OR, USA) and 5% Neurobiotin (Vector, UK) in saline or KCl (pH 6.5). At the conclusion of the experiments, a lethal dose of pentobarbital was administered to the animals and they were perfused, initially with physiological saline and subsequently with paraformaldehyde (4%) in 0.1 M phosphate buffer. Blocks of lumbar spinal cord containing labelled cells were removed and placed initially in the same fixative (for 8 h at 4°C) and then in phosphate buffer or in 30% sucrose in phosphate buffer.

Experimental procedures on rats

Surgical procedures. Four adult male Sprague–Dawley rats (250–350 g) were deeply anaesthetized with an intraperitoneal injection of ketamine and xylazine (2:1 0.1 ml (100 g)$^{-1}$) and placed in a stereotaxic frame under strict aseptic conditions. The skin at the back of the head was cut in the midline and the skull was exposed. A small burr hole was then made on the left-hand side at inter-aural co-ordinates –4.2 mm (anterior–posterior) and –2.0 mm (medio-lateral) (Paxinos & Watson, 1997). A glass micropipette with a tip diameter of 20 μm filled with 0.2 μl cholera toxin b subunit (CTb, 1%) (Sigma-Aldrich, Co., Poole, UK) in distilled water was aligned with the burr hole and inserted into the cerebellum at a dorso-ventral co-ordinate of +4.5. CTb (200 nl) was injected by pressure with a Pico injector (World Precision Instruments, Sarasota, USA). The micropipette was left in place for 5 min after injection to prevent backflow of tracer and then removed. The exposed surface was then sutured and the animals recovered from anaesthesia usually within 2–4 h, displaying exploratory behaviour and starting to drink. Following a 6 day post-operative survival period, the animals were re-anaesthetized with pentobarbitone (1 ml 200mg/ml I.P.) and perfused with saline followed by 4% paraformaldehyde in 0.1 M phosphate buffer through the left ventricle. The spinal cord and brain were removed

Table 1. Summary of the primary and secondary antibody combinations and concentrations used in the current study

	Primary antibody combination	Primary antibody concentration	Supplier	Secondary antibody combination	Secondary antibody concentration	Supplier
Cat	Guinea pig/rabbit VGLUT1	1:5000	Chemicon/Synaptic systems	Cy-5	1:100	Jackson ImmunoResearch
	Rabbit VGLUT2	1:5000	Chemicon	Alexa 488	1:500	Molecular Probes
Rat	Mouse CTb	1:250	A. Wikström, University of Gothenburg	Rh. Red	1:100	Jackson ImmunoResearch
	Guinea pig VGLUT1	1:5000	Chemicon	Cy-5	1:100	Jackson ImmunoResearch
	Rabbit VGLUT2	1:5000	Chemicon	Alexa 488	1:500	Molecular Probes

All secondary antibodies were raised in donkey and conjugated to: Rh. Red, Rhodamine Red; Cy-5, Cyanine 5.18; Alexa 488, Alexa Fluor 488; CTb, b-subunit of cholera toxin; VGLUT, vesicular glutamate transporter.

and post-fixed in the same fixative for 8 h at 4°C. The cerebellum and brainstem were kept in fixative for 1–2 days and cut coronally at 100 μm using freezing microtome for histological examination of the injection site.

Identification of injection sites. Injection sites were visualized by using 3,3′-diaminobenzidine (DAB) as a chromogen. Sections were incubated in goat anti-CTb for 48 h followed by biotinylated anti-goat IgG for 3 h at room temperature. Sections were then incubated in avidin–horseradish peroxidase (HRP) for 1 h and hydrogen peroxide plus DAB was applied for a period of approximately 15 min to reveal immunoreactivity at injection sites. Sections were then mounted on gelatin-coated slides and were dehydrated, cleared and a coverslip was applied. Injection sites were viewed with transmission light microscopy and photographed digitally (AxioVision 4.8 software, Zeiss, Germany). The location of the injection site was determined with reference to the stereotaxic rat brain atlas of Paxinos & Watson (1997).

Immunohistochemical procedures. L3–L6 segments of the cat and Th12–L3 segments of the rat were cut into 50-μm-thick transverse sections with a Vibratome (Oxford Instruments, Technical Products International Inc., USA) after which they were placed immediately in an aqueous solution of 50% ethanol for 30 min to enhance antibody penetration. Thereafter the sections were washed several times with 0.1 M phosphate-buffered saline that contained 0.3 M NaCl (PBS) and mounted with anti-fade medium, Vectashield (Vector Laboratories, Peterborough, UK) on glass slides.

Cat sections were collected and mounted in strict serial order to enable reconstruction of the labelled cells and mounted in the same serial order. The sections were examined for labelled spinocerebellar neurons with a fluorescence microscope and those containing labelled neurons were washed several times in PBS. They were then incubated in avidin–rhodamine (1:1000, Jackson ImmunoResearch, Luton, UK) for 3 h and mounted in Vectashield on glass slides. Sections were re-scanned using a fluorescence microscope and those containing well-labelled neurons were processed for immunocytochemistry. Selected sections containing intracellularly labelled neurons were washed firstly several times in PBS and then incubated in a combination of the following primary antibodies: guinea pig anti-VGLUT1 and rabbit anti-VGLUT2 for 72 h at 4°C. Following several washes in PBS, the sections were incubated in a combination of secondary antibodies coupled to cyanine 5.18 and Alexa 488 for 3 h at room temperature to identify VGLUT1 and VGLUT2 terminals, respectively. They were then rinsed in PBS and mounted in Vectashield. All antibodies were diluted in PBS containing 0.3% trition (PBST) (see Table 1 for details of antibodies used).

Retrogradely labelled rat spinocerebellar neurons were identified by the presence of CTb transported from injection sites and grouped into different populations based on their anatomical locations. Three-colour immunofluorescence was performed on these sections with guinea pig anti-VGLUT1 and rabbit anti-VGLUT2 antibodies (see rat sections in Table 1) using the same procedures as for cat neurons. In both series of experiments, the sections were scanned using three channels of a confocal laser scanning microscope (BioRad Radiance, Hemmel Hempstead, UK). VGLUT1-immunoreactive terminals were imaged as blue, while VGLUT2 terminals were green.

Confocal microscopy, reconstruction and analysis. Sections containing cell bodies and dendrites of intracellularly labelled cat neurons were initially scanned at low power (×20 lens, zoom factor 1.2) and this image was used as a frame of reference for the location of labelled processes within each section and to make preliminary reconstructions of the cells. Following this, individual cells were scanned at a higher magnification using a ×40 oil immersion lens at zoom factor of 2 at an increment of 0.5 μm. Series of confocal images were gathered and a montage was constructed for each cell. Usually the processes of cells extended within six or seven sections and 60–80 series of images were collected from each section.

Cells were reconstructed three dimensionally by using Neurolucida for Confocal software (MicroBrightField, Colchester, VT, USA) and VGLUT1 and VGLUT2 contacts on the labelled cells were mapped. Reconstructions were always started from the stacks of single optical sections containing the cell body. Once the reconstruction of the cell body was complete, dendritic processes were systematically added and contacts were plotted and recorded simultaneously with appropriate markers from the subsequent stacks until reconstruction of the dendritic tree was complete. Only contacts in close apposition with the cell in the same focal plane and with no intervening black pixel space were counted.

Once the three-dimensional reconstruction of the cell was complete and the contacts were recorded, contact densities were calculated using data generated by Neurolucida and expressed as numbers of contacts per unit area (100 μm^2) of neuronal surface. The surface area of the cell body was estimated by measuring the perimeter of each labelled cell body from projected confocal images by using ImageJ software (National Institutes of Health, USA) and calculating the surface area of an equivalent sphere. The distribution of contacts was analysed using Sholl analysis with Neurolucida Explorer. The number of contacts within series of 25 μm concentric spheres from the centre of the cell body of each cell was expressed as numbers per 100 μm of dendritic length. Numbers of contacts within each sphere were averaged for the four types of cell and shown as Sholl plots.

Retrogradely labelled rat spinocerebellar neurons were examined ipsilaterally to the injection site. Sections from Th12 to L3 segments were firstly scanned at low power (×10 lens, zoom factor 1) and these images was used as a frame of reference to categorize the neurons into different populations based on their anatomical location in the spinal cord grey matter. Sections containing well-labelled neurons were then scanned with the confocal microscope by using a ×40 oil immersion lens with a zoom factor of 2 at 0.5 μm intervals. The stacks of images obtained were analysed with Neurolucida for Confocal software. Reconstructions of cells were made and VGLUT1 and VGLUT2 contacts on the labelled cells were plotted on them. Analysis of the contacts formed with these spinocerebellar neurons was performed in the same way as described above for the intracellularly labelled neurons.

Statistical analysis

Data were expressed as mean ± standard deviation (SD). Multi-group comparisons were made by using an analysis of variance test (ANOVA) followed by a *post hoc* Tukey's analysis as appropriate and two variable comparisons among the same population was made by using Student's *t* test. A $P < 0.05$ was considered to be statistically significant.

Results

Glutamatergic terminals on intracellularly labelled cat neurons

In total, a sample of 22 well-labelled spinocerebellar neurons that showed no evidence of damage following the injection of the markers was used for quantitative comparison of the numbers of glutamatergic terminals. The neurons included six SB neurons (cells 1–6), three VSCT neurons (cells 7–9), three ccDSCT neurons (cells 10–12) and three dhDSCT neurons (cells 13–15) for comparison of distribution of VGLUT1 and VGLUT2 contacts on the same cells. An additional seven cells were analysed for VGLUT1 contacts only (cells a–g); these were three ccDSCT, three dhDSCT and one VSCT cells used for inter-population comparisons on the whole sample of neurons.

Individual neurons antidromically activated from within or close to the nucleus interpositus were classified into four subpopulations on the basis of coupling between primary afferents and these neurons, and according to their anatomical location in the lumbar grey matter, as described in the Methods. Electrophysiological recordings from four neurons representative of the two populations of the VSCT and the two populations of the DSCT neurons are shown in Fig. 1. The records illustrate antidromic activation from the cerebellum (in the middle panels) of all of these neurons. Furthermore, they illustrate strong inhibition from muscle afferents from the quadriceps nerve in SB (cell 3) and VSCT (cell 8) neurons and a lack of excitatory input from this nerve in the majority of SB neurons and some VSCT neurons (in the left panels). Peripheral excitatory input from the tested muscle nerves was not detected in 5 of the 6 SB neurons whereas excitatory input from at least one muscle nerve was evoked in all VSCT neurons. The records also illustrate the much

shorter latencies of excitation of ccDSCT neurons (cell 12) following quadriceps stimulation when compared with dhDSCT (cell 13) neurons; these were compatible with actions evoked by group I and group II afferents, respectively.

The locations of cell bodies of these neurons are indicated in Fig. 2. Cell bodies of SB neurons (red circles) were located within the most lateral part of the grey matter in lamina VII while cell bodies of VSCT neurons (green circles) were within more medial parts of lamina VII. The cell bodies of ccDSCT neurons (purple circles) were located within Clarke's column whereas dhDSCT neurons (blue circles) had their cell bodies in either lamina V or VI. The locations of the cell bodies of the 15 cells which were analysed for both VGLUT1 and VGLUT2 are indicated by filled circles whereas open circles indicate locations of the cell bodies of the 7 cells analysed for VGLUT1 only. Both the location and morphology of the labelled neurons was fully consistent with the classification of these cells based on their input.

To what extent is excitatory input to different populations of spinocerebellar neurons monosynaptic from primary afferents and to what extent it is from other neurons?

As specified in the Introduction, immunoreactivity against vesicular glutamate transporter 1 (VGLUT1) or vesicular glutamate transporter 2 (VGLUT2) was used as an indication of peripheral afferent or central origin of the terminals in contact with the labelled neurons (see Discussion for an evaluation of this rationale). The results summarised in Table 2 and illustrated in Figs 3–5 reveal strikingly different patterns of VGLUT1 and VGLUT2 axonal contacts on SB, VSCT, ccDSCT and dhDSCT neurons. Examples of confocal microscope images revealing immunocytochemical properties of axon terminals contacting labelled neurons (one from each group) are shown in Fig. 3*A*, *B*, *C* and *D*, respectively.

Figure 3*A* shows confocal microscope images of VGLUT2-immunoreactive axon terminals in contact with the cell body and dendritic trunk of a SB neuron

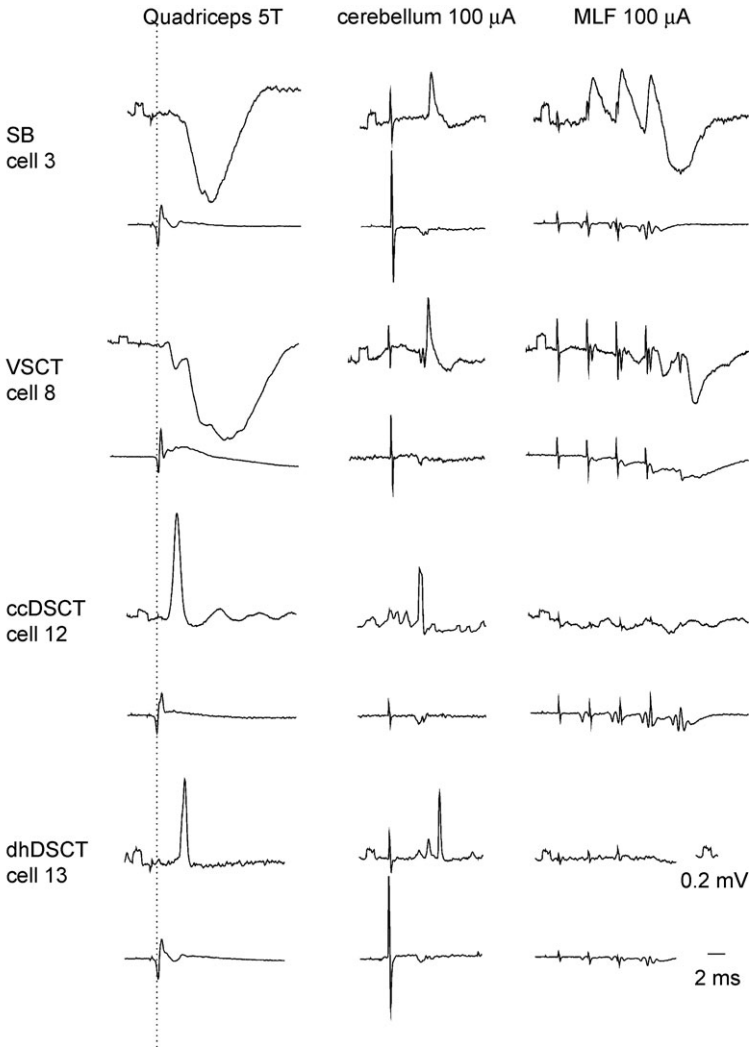

Figure 1. Representative examples of PSPs used to identify the four different populations of lumbar spinocerebellar neurons analysed morphologically
In each pair of traces, the upper trace is an intracellular record from the cell indicated (negativity downward) and the lower trace is from the cord dorsum (negativity upward). All of the illustrated postsynaptic potentials in the left column were evoked by stimuli applied to the quadriceps nerve at 5 times threshold (5T). The dotted line indicates the afferent volleys. All rectangular calibration pulses at the beginning of traces are 0.2 mV.

Table 2. The number and densities of VGLUT1 and VGLUT2 axon terminals in apposition with the cell bodies and dendrites of different populations of intracellularly labelled spinocerebellar tract neurons in cats

				Soma					Dendrite					
Populations of spinocerebellar tract neurons	Cell	Contacts (total number)		Contacts (*n*)		Surface area (μm^2)	Density (*n*/100 μm^2)		Contacts (*n*)		Total dendritic length (μm)	Surface area (μm^2)	Density (*n*/100 μm^2)	
		VGLUT1	VGLUT2	VGLUT1	VGLUT2		VGLUT1	VGLUT2	VGLUT1	VGLUT2			VGLUT1	VGLUT2
SB	—	—	—	—	—	—	—	—	—	—	—	—	—	—
	Cell 1	43	4413	5	148	14214.43	0.04	1.04	38	4265	15639.80	137176.29	0.03	3.11
	Cell 2	52	5006	0	85	22147.44	0.00	0.38	52	4921	13857.60	135472.01	0.04	3.63
	Cell 3	18	3461	0	119	18231.61	0.00	0.65	18	3342	10494.30	117120.97	0.02	2.85
	Cell 4	29	3350	4	127	10151.65	0.04	1.25	25	3223	12178.20	95415.10	0.03	3.38
	Cell 5	36	4998	0	140	11333.18	0.00	1.24	36	4858	21372.70	171956.71	0.02	2.83
	Cell 6	25	4605	0	170	9853.31	0.00	1.73	25	4435	17415.00	145863.22	0.02	3.04
Mean	—	—	—	—	—	—	**0.01**	**1.05**	—	—	—	—	**0.02**	**3.14**
SD	—	—	—	—	—	—	**0.02**	**0.48**	—	—	—	—	**0.01**	**0.31**
VSCT	—	—	—	—	—	—	—	—	—	—	—	—	—	—
	Cell 7	451	2057	24	20	15813.27	0.15	0.13	427	2037	10821.80	88947.60	0.48	2.29
	Cell 8	843	3731	110	208	23494.96	0.47	0.89	733	3523	16532.80	237681.10	0.31	1.48
	Cell 9	185	4132	5	90	14158.38	0.04	0.64	180	4042	1894.50	136782.27	0.13	2.96
	Cell a*	627	—	16	—	14947.19	0.11	—	497	—	4874	53863.5	0.92	—
Mean	—	—	—	—	—	—	**0.19**	**0.55**	—	—	—	—	**0.46**	**2.24**
SD	—	—	—	—	—	—	**0.19**	**0.39**	—	—	—	—	**0.34**	**0.74**
ccDSCT	—	—	—	—	—	—	—	—	—	—	—	—	—	—
	Cell 10	1213	24	27	2	10804.80	0.25	0.02	1186	22	2504.90	44898.72	2.64	0.05
	Cell 11	721	45	6	5	4567.81	0.13	0.11	715	40	2166.70	25711.70	2.78	0.16
	Cell 12	1708	162	85	1	9317.87	0.91	0.01	1623	161	2805.50	53763.82	3.02	0.30
	Cell b*	1245	—	20	—	5859.13	0.34	—	686	—	2188.9	25757.44	2.66	—
	Cell c*	1355	—	57	—	7118.77	0.80	—	827	—	3624.5	49684.52	1.66	—
	Cell d*	3049	—	78	—	15951.52	0.49	—	1238	—	7667.2	82986.78	1.49	—
Mean	—	—	—	—	—	—	**0.49**	**0.05**	—	—	—	—	**2.38**	**0.17**
SD	—	—	—	—	—	—	**0.31**	**0.05**	—	—	—	—	**0.64**	**0.13**
dhDSCT	—	—	—	—	—	—	—	—	—	—	—	—	—	—
	Cell 13	1082	403	7	29	6404.21	0.11	0.45	1075	374	5630.80	55767.37	1.93	0.67
	Cell 14	2276	1211	267	90	14347.69	1.86	0.63	2009	1121	9198.60	90628.60	2.22	1.24
	Cell 15	1291	1274	52	111	12466.69	0.42	0.89	1239	1163	10979.20	98521.86	1.26	1.18
	Cell e*	1137	—	29	—	10127.78	0.29	—	1061	—	6016.4	56847.3	1.87	—
	Cell f *	2221	—	87	—	16828.68	0.52	—	1997	—	8841.8	98492.42	2.03	—
	Cell g*	2058	—	37	—	16924.57	0.22	—	2014	—	9829.3	100458.97	2.00	—
Mean	—	—	—	—	—	—	**0.57**	**0.66**	—	—	—	—	**1.88**	**1.03**
SD	—	—	—	—	—	—	**0.65**	**0.22**	—	—	—	—	**0.33**	**0.31**

*Neurons analysed for VGLUT1 only.

(cell 1). Few VGLUT1-positive axon terminals contacted this or other SB cells. In contrast, both VGLUT1- and VGLUT2-positive terminals were found in contact with the cell body and dendrites of VSCT neurons, as illustrated in Fig. 3*B* (cell 8). Although both kinds of contacts were also found on ccDSCT and dhDSCT neurons, for most DSCT neurons the majority of the contacts were formed by VGLUT1 terminals and, in the case of ccDSCT neurons, very few contacts were formed by VGLUT2 axon terminals. Figure 3*C* and *D* show confocal microscope images of

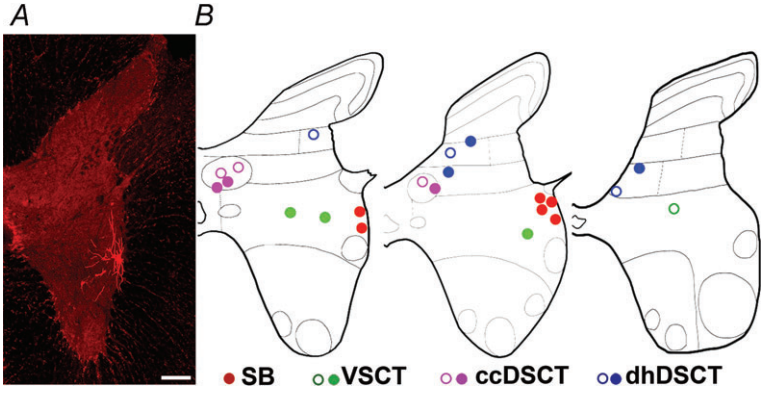

Figure 2. Locations of 22 intracellularly labelled spinocerebellar neurons
A, a low-magnification image of a transverse section of the L3 segment of the spinal cord showing the location of one of the SB neurons (cell 5). *B*, diagrams illustrating the locations of cell bodies of all 22 cells in L3, L4 and L5 segments, respectively. Filled circles indicate location of the 15 cells which were analysed for both VGLUT1 and VGLUT2 while the open circles are for the 7 additional cells which were analysed for VGLUT1 only. Scale bar in *A*, 200 μm.

VGLUT1- and VGLUT2-immunoreactive axon terminals in contact with the cell body and dendritic trunk of a ccDSCT neuron (cell 10) and a dhDSCT neuron (cell 14), respectively. Figure 3*C* also illustrates the much lower density of VGLUT2 labelling within Clarke's column than in the neuropil just ventral to it. Generally Fig. 3 illustrates that there is a good correspondence between the density of VGLUT1- and VGLUT2-positive terminals associated with the analysed spinocerebellar neurons and the concentration of these terminals within the regions of the grey matter where they are located (Alvarez *et al.* 2004).

The differences in the number of VGLUT1- and VGLUT2-positive terminals in contact with the four

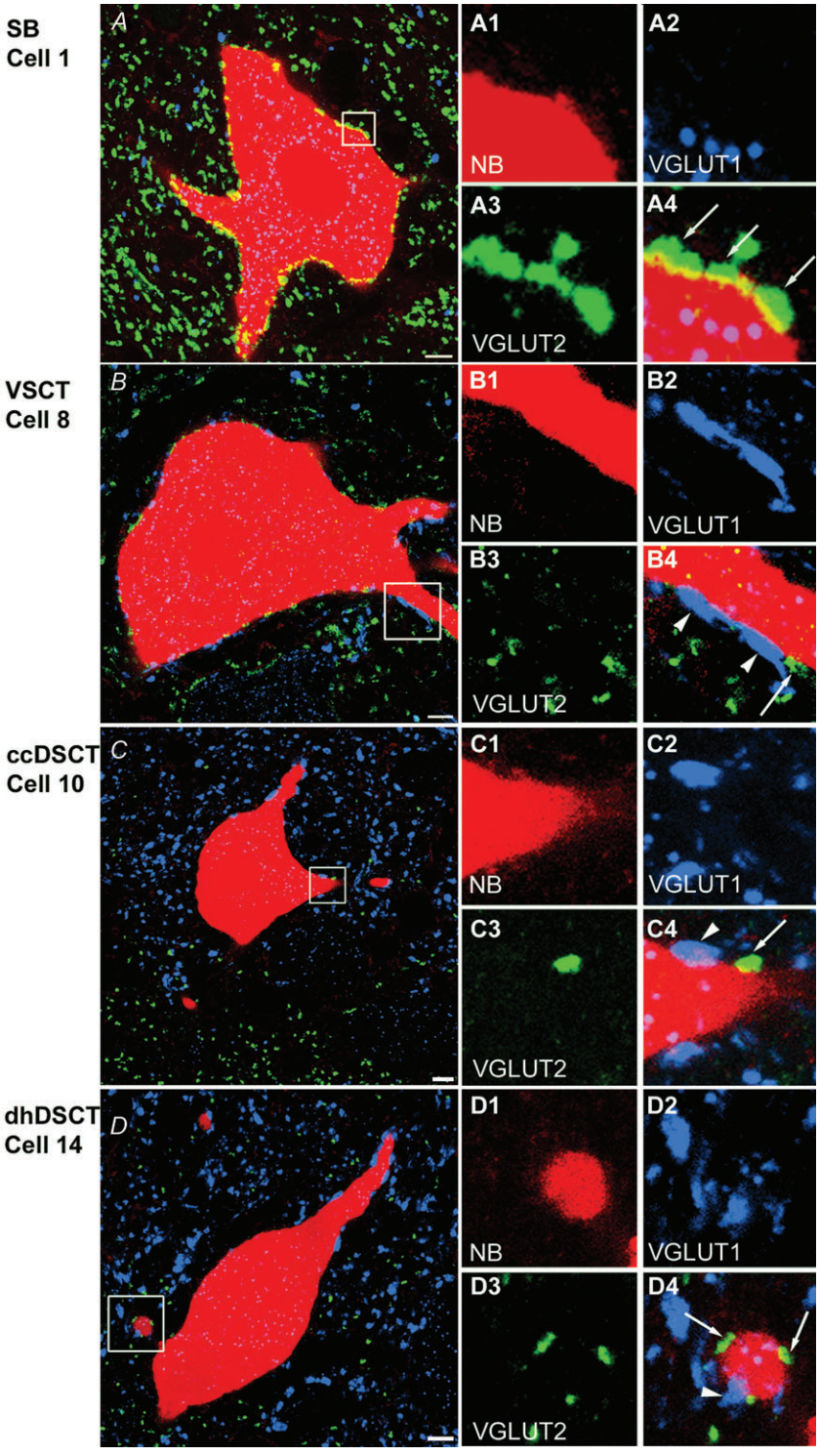

Figure 3. Immunohistochemical characteristics of VGLUT1 and VGLUT2 axon terminals in contact with intracellularly labelled spinocerebellar neurons
A–D, single optical sections through the cell bodies of representative SB (Cell 1), VSCT (Cell 8), ccDSCT (Cell 10) and dhDSCT (Cell 14) neurons showing the presence of VGLUT1 (blue) and VGLUT2 (green) immunoreactive boutons. The cell body and dendrites of intracellularly labelled cells are in red. *A*1–*A*4, *B*1–*B*4, *C*1–*C*4 and *D*1–*D*4, images of dendritic trunks from cells shown in *A, B, C* and *D*, respectively (areas encompassed in the boxes) illustrating contacts made by VGLUT1- and VGLUT2-immunoreactive boutons with the cell indicated by arrowheads and arrows, respectively. Note differences in the density of VGLUT1- and VGLUT2-immunoreactive terminals within different regions of the grey matter shown in *A–D* and especially the high density of VGLUT1 and low density of VGLUT2 within Clarke's column shown in *C*. Scale bar in *A–D*, 10 μm.

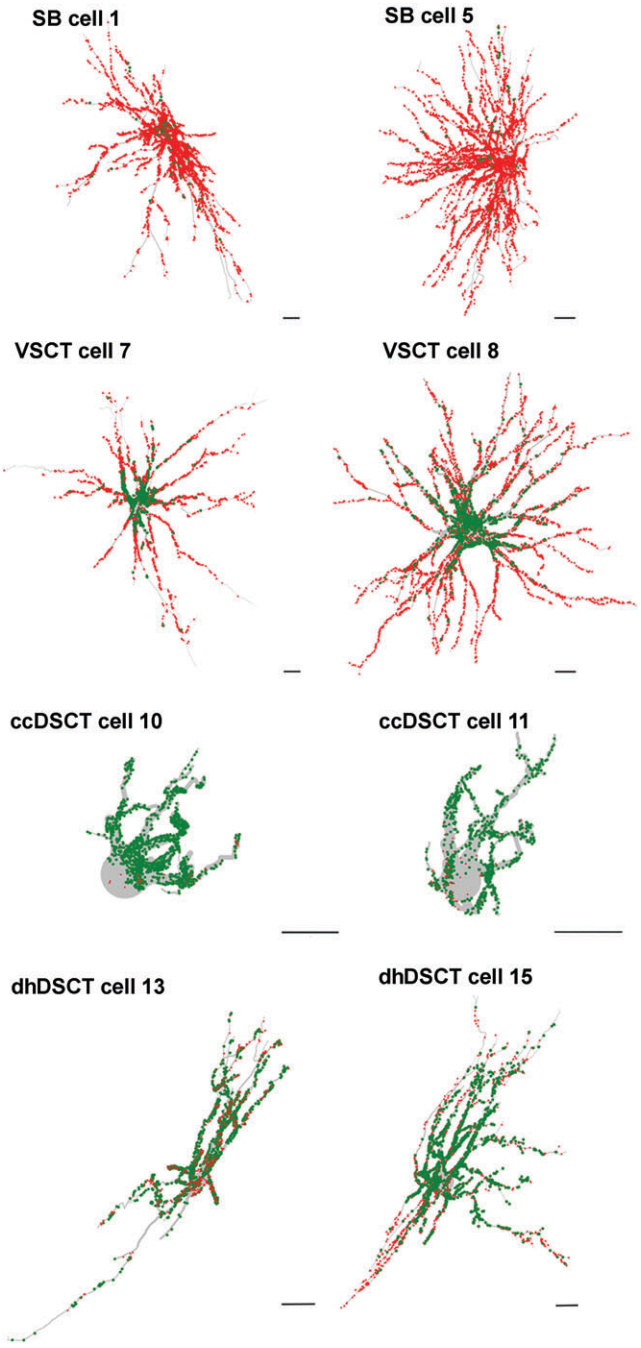

Figure 4. Reconstructions of spinocerebellar tract neurons illustrating the four different types of distribution patterns of VGLUT1 and VGLUT2 contacts
Reconstructions of spinocerebellar tract neurons showing the distributions of VGLUT1 (green) and VGLUT2 (red) contacts throughout the dendritic trees. The reconstructions were made with Neurolucida for Confocal software. Cell body and dendrites are shown in light grey. Scale bars, 50 μm. All are oriented such that the midline is to the left and the lateral borders of the grey matter to the right, as in Fig. 2.

populations of spinocerebellar neurons became even more marked when overall distribution of these terminals on the soma and along the whole dendritic tree of the four populations of spinocerebellar neurons was compared. Reconstructions of the distribution of VGLUT1- and VGLUT2-immunoreactive axon terminals are shown in Fig. 4 for two cells of each population.

These reconstructions illustrate: (i) that VGLUT2 contacts are distributed on both somata and dendrites of SB neurons; (ii) that the overwhelming majority of VGLUT1 contacts are on somata of VSCT neurons while VGLUT2 contacts are concentrated on dendrites, especially distally; (iii) that VGLUT1 contacts are distributed on both somata and dendrites of ccDSCT neurons; and (iv) that mixed VGLUT1 and VGLUT2 contacts are distributed on both somata and dendrites of dhDSCT neurons.

Quantitative comparison of coverage of VGLUT1 and VGLUT2 on intracellularly labelled SB and VSCT neurons

A quantitative analysis of the density of VGLUT1 and VGLUT2 terminals associated with cell bodies and dendrites was performed for each class of cell of our main sample. The results are summarized in Table 2 and in Fig. 5*A* and *B*. The overall average density (i.e. on both soma and dendrites) calculated per 100 μm^2 of SB neurons was more than 200 times lower for VGLUT1 than for VGLUT2 contacts (0.02 ± 0.01 and 2.92 ± 0.25, respectively). This difference was statistically highly significant (Student's t test, $P < 0.0001$). For VSCT neurons the average contact density per 100 μm^2 was only about 10 times lower for VGLUT1 than for VGLUT2 contacts (0.29 ± 0.16 and 2.04 ± 0.66, respectively) but this difference was also statistically significant (Student's t test, $P < 0.005$).

Comparison of the overall coverage densities on SB and VSCT neurons revealed a weak statistically significant difference for VGLUT2 boutons ($P < 0.05$; ANOVA), the density being on average 1.5–2 times higher on SB neurons. No statistically significant difference ($P > 0.05$) was found between the overall densities of VGLUT1 contacts on these two populations of VSCT neurons even though the average density of VGLUT1 contacts on VSCT neurons was 15 times higher than on SB neurons.

Quantitative comparison of coverage of VGLUT1 and VGLUT2 on two functional populations of intracellularly labelled DSCT neurons

In ccDSCT neurons, the overall average density of VGLUT1 per 100 μm^2 was more than 10 times higher than VGLUT2 contacts (2.42 ± 0.27 and 0.15 ± 0.11, respectively). This difference was statistically significant

(Student's t test, $P < 0.0001$). In the dorsal horn population of DSCT neurons (dhDSCT), the overall average surface density of VGLUT1 was less than two times higher than of VGLUT2 contacts (1.69 ± 0.50 and 0.98 ± 0.29, respectively). Also this difference was statistically significant (Student's t test, $P < 0.02$).

Differences in the overall contact density of VGLUT2 terminals on ccDSCT and dhDSCT neurons were not found to be statistically significant but ccDSCT neurons showed significantly higher number of VGLUT1 contacts ($P < 0.05$). Diagrams in Fig. 5*A* and *B* also show that the overall contact density of VGLUT1 terminals was significantly higher on ccDSCT neurons than on dhDSCT, VSCT or SB neurons and that the overall contact density of VGLUT2 terminals was significantly higher on SB than on VSCT, dhDSCT or ccDSCT neurons.

The density of VGLUT1 and VGLUT2 contacts for individual neurons given in Table 2 and a Sholl analysis for the four types of cell in Fig. 6 provide a quantitative measure of the differences illustrated in Fig. 4. Both the table and Sholl analysis show that much higher proportions of VGLUT2 relative to VGLUT1 terminals were found on somata and dendrites of SB and VSCT neurons, although differences in the densities were greater

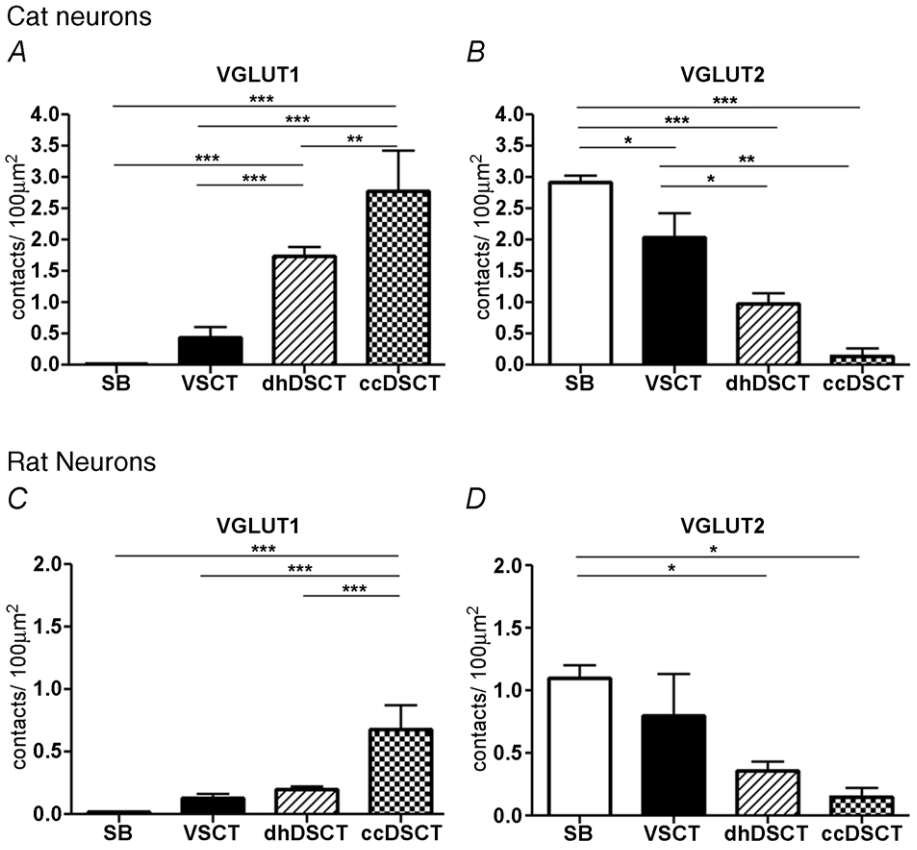

Figure 5. Comparison between the contact density of VGLUT1 and VGLUT2 axon terminals in different populations of spinocerebellar neurons
A, differences in the overall contact density of VGLUT1 boutons per 100 μm^2 for the four different populations of spinocerebellar neurons in the cat. The contact density in ccDSCT neurons is significantly different from that on dhDSCT neurons ($P < 0.01$), VSCT neurons ($P < 0.001$) and SB neurons ($P < 0.001$). Similarly, the overall contact density on dhDSCT neurons is significantly different from that of VSCT neurons ($P < 0.001$) and SB neurons ($P < 0.001$). *B*, differences in the contact density of VGLUT2 boutons per 100 μm^2 in different populations of spinocerebellar neurons in the cat. The contact density in SB neurons is significantly different than in VSCT ($P < 0.05$), dhDSCT ($P < 0.001$) and ccDSCT ($P < 0.001$) neurons. The contact density on VSCT neuron is also significantly different from dhDSCT ($P < 0.05$) and ccDSCT ($P < 0.001$) neurons. *C*, differences in the overall contact density of VGLUT1 boutons per 100 μm^2 in four different populations of spinocerebellar neurons in the rat. The contact density in the ccDSCT neurons is significantly different from that on dhDSCT neurons ($P < 0.001$), VSCT neurons ($P < 0.001$) and SB neurons ($P < 0.001$). *D*, differences in the contact density of VGLUT2 boutons per 100 μm^2 in different populations of spinocerebellar neurons in the rat. The contact density in SB neurons is significantly different than in dhDSCT ($P < 0.05$) and ccDSCT ($P < 0.05$) neurons. $^*P < 0.05$, $^{**}P < 0.01$ and $^{***}P < 0.001$.

on the dendrites when compared with somata (about 150 times *vs.* 100 times for SB neurons and about 7 times *vs.* 2.5 times for VSCT neurons). Synaptic actions of VGLUT2 terminals therefore may be evoked within all compartments of the dendritic trees of SB and VSCT neurons whereas actions of VGLUT1 terminals are focused upon proximal dendrites. Differences in densities of VGLUT1 and VGLUT2 terminals on ccDSCT neurons likewise were more apparent on dendrites than on somata (about 16 times *vs.* 8 times) but the differences on somata were found in only 2 out of 3 cells. These differences were even smaller on dendrites of dhDSCT neurons (about 2 times, in 2 out of 3 cells), and were not apparent on somata.

Taken together our results indicate that the distribution of VGLUT1 and VGLUT2 contacts within each class of cat spinocerebellar neuron is characteristic and differs from the distribution in other classes.

Glutamatergic terminals on retrogradely labelled rat neurons

A representative example of a CTb injection site in the cerebellum is shown in Fig. 7. The 80 spinocerebellar tract neurons analysed in rats included 24 ccDSCT neurons, 21 dhDSCT neurons, 18 SB neurons and 17 VSCT neurons. The first criterion for selection was strong labelling of both cell bodies and dendritic trees at distances of at least 35 μm from the soma (average distance of 164.23 μm). The second criterion was a location equivalent to the location of intracellularly labelled spinocerebellar neurons in cat. As shown in Fig. 8, SB neurons were classified as those with cell bodies located within the most lateral part

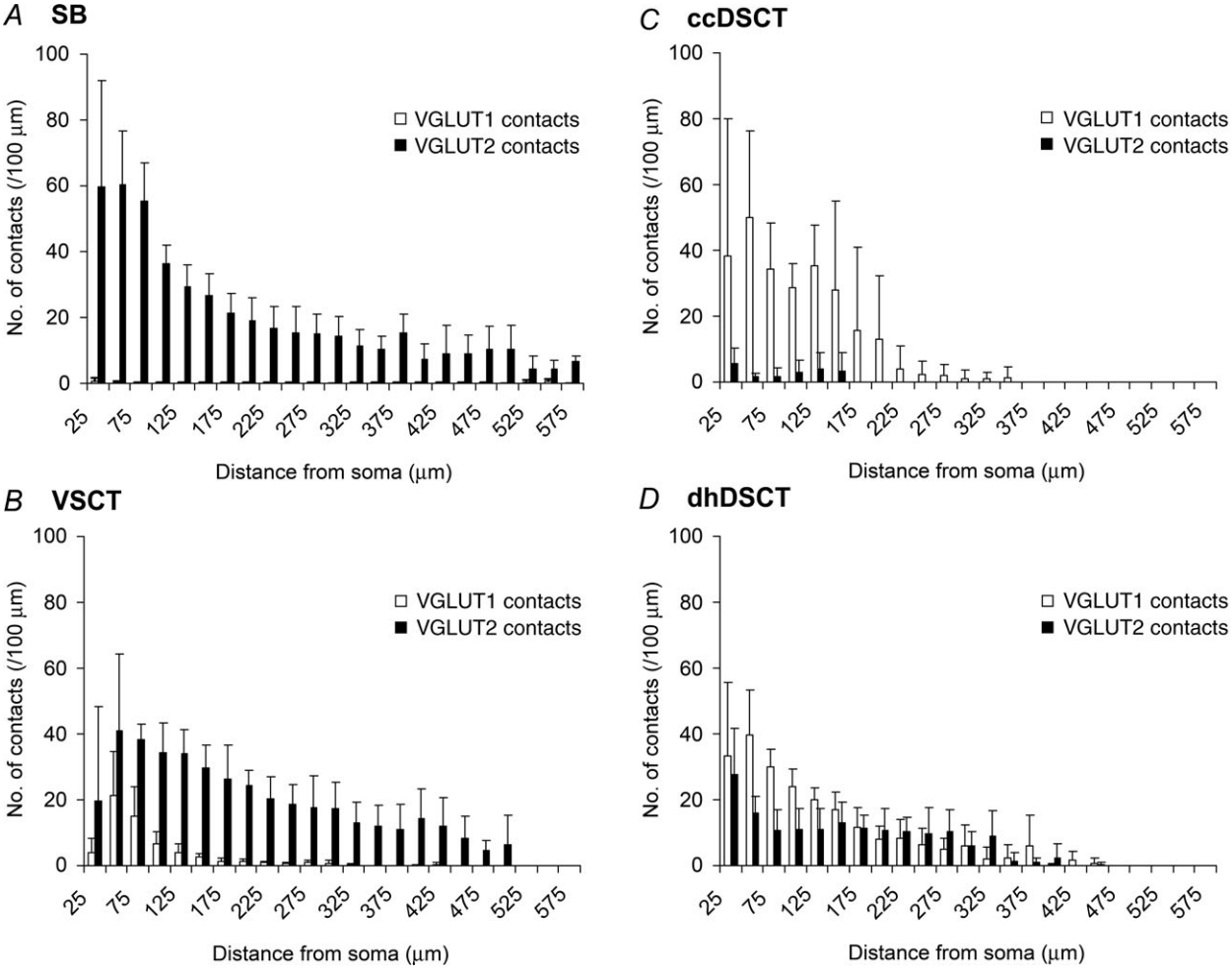

Figure 6. Bar charts derived from Sholl analysis
Comparison of the mean numbers of VGLUT1 and VGLUT2 terminals forming contact with different populations of intracellularly labelled spinocerebellar tract neurons: *A*, SB neurons (cells 1 to 6); *B*, VSCT neurons (cells 7 to 9 and cell a); *C*, ccDSCT neurons (cells 10 to 12 and cells b to d); and *D*, dhDSCT neurons (cells 13 to 15 and cells e to f). The plots show the mean numbers of contacts per 100 μm of dendritic length contained within concentric spheres with radii which increase in 25 μm from the centre of the cell body. Bars represent the standard deviations.

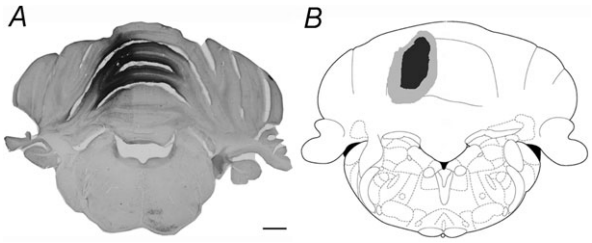

Figure 7. Photomicrograph and reconstruction of a representative section of the brain illustrating an injection site in the cerebellum
A, a photomicrograph of a coronal section of the brain showing an injection site in the cerebellum. *B*, the black shaded area shows the CTb injection site and the grey shaded area shows the maximum spread of the CTb projected on a schematic drawing based on the atlas of Paxinos & Watson (1997). Scale bar in *A*, 100 μm.

of the grey matter in lamina VII (red circles) and VSCT neurons as those located within more medial parts of lamina VII (green circles). Likewise, ccDSCT and dhDSCT neurons were classified as those located within Clarke's column (purple circles) or outside Clarke's column in either lamina V or VI (blue circles).

Examples of confocal microscope images for each of these neuronal populations are shown in Fig. 9. As in the cat, they illustrate the preferential contacts of VGLUT2-immunoreactive contacts on SB neurons and the location of these neurons within the region of the grey matter with a much higher density of VGLUT2- than VGLUT1-immunoreactive terminals. In contrast, ccDSCT neurons show preferential VGLUT1-immunoreactive contacts and are located within a region of the grey matter with a much higher density of VGLUT1- than VGLUT2-immunoreactive terminals.

Quantitative comparison of coverage of VGLUT1 and VGLUT2 on retrogradely labelled SB and VSCT neurons

A quantitative comparison of the density of VGLUT1- and VGLUT2-immunoreactive terminals contacting SB

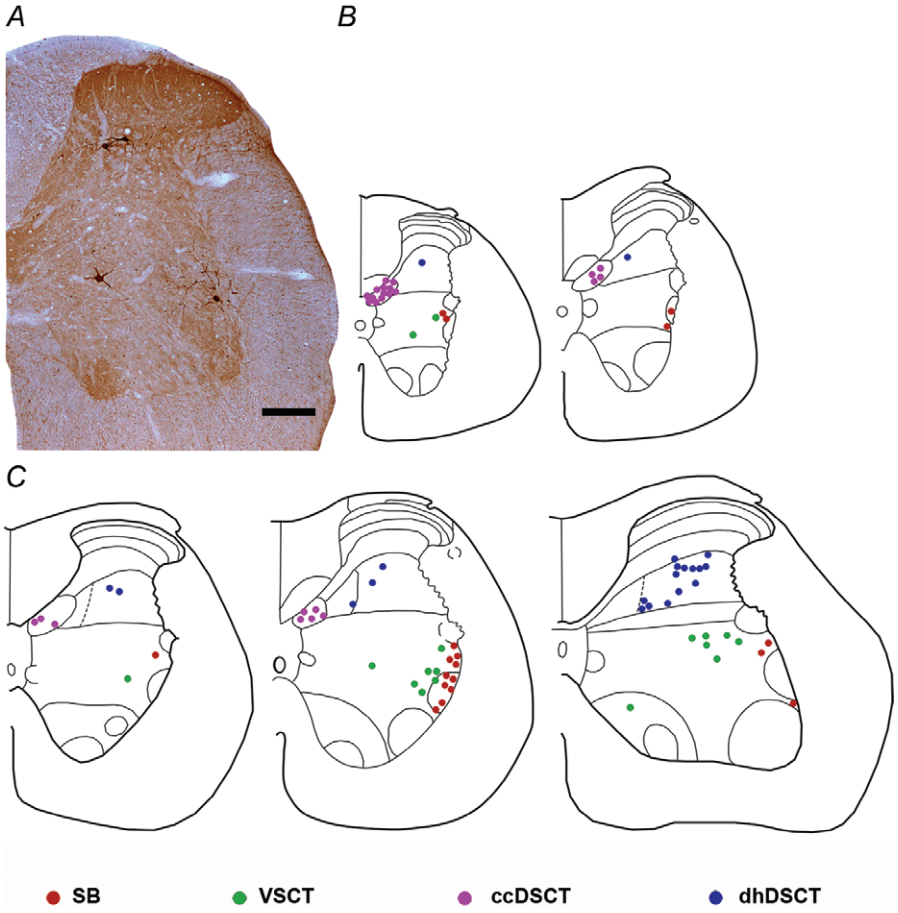

Figure 8. Locations of 80 analysed spinocerebellar neurons labelled retrogradely
A, a photomicrograph of a transverse section of the L3 segment of the rat spinal cord showing the location of one of the SB neurons, VSCT neurons and dhDSCT neurons identified by retrograde transport of CTb. *B* and *C*, diagrams illustrating the locations of cell bodies of 80 cells analysed in the Th12 and Th13 segments and L1, L2 and L3 segments, respectively. Scale bar in *A*, 20 μm.

neurons reveals a significantly higher density of VGLUT2 contacts in comparison to VGLUT1 contacts (Student's *t* test, $P < 0.0001$). The overall average density of VGLUT1 and VGLUT2 contacts calculated per 100 μm^2 of SB neurons was 0.02 ± 0.01 and 1.10 ± 0.21, respectively. In contrast, the average overall densities of VGLUT1 and VGLUT2 contacts on VSCT neurons were 0.13 ± 0.04 and 0.80 ± 0.64 per 100 μm^2, respectively. This difference was also statistically significant (Student's *t* test, $P < 0.05$).

Although these VSCT neurons have a higher number of VGLUT1 contacts relative to SB neurons, comparison of the overall contact densities on SB and VSCT was not significantly different ($P > 0.05$; ANOVA see Fig. 5*C* and *D*). Similarly, no statistically significant difference ($P > 0.05$; ANOVA) was found between the overall contact density of VGLUT2 on these two populations of neurons.

Quantitative comparison of coverage of VGLUT1 and VGLUT2 on retrogradely labelled ccDSCT and dhDSCT neurons

The overall average density of VGLUT1 and VGLUT2 contacts on ccDSCT neurons was 0.68 ± 0.19 and

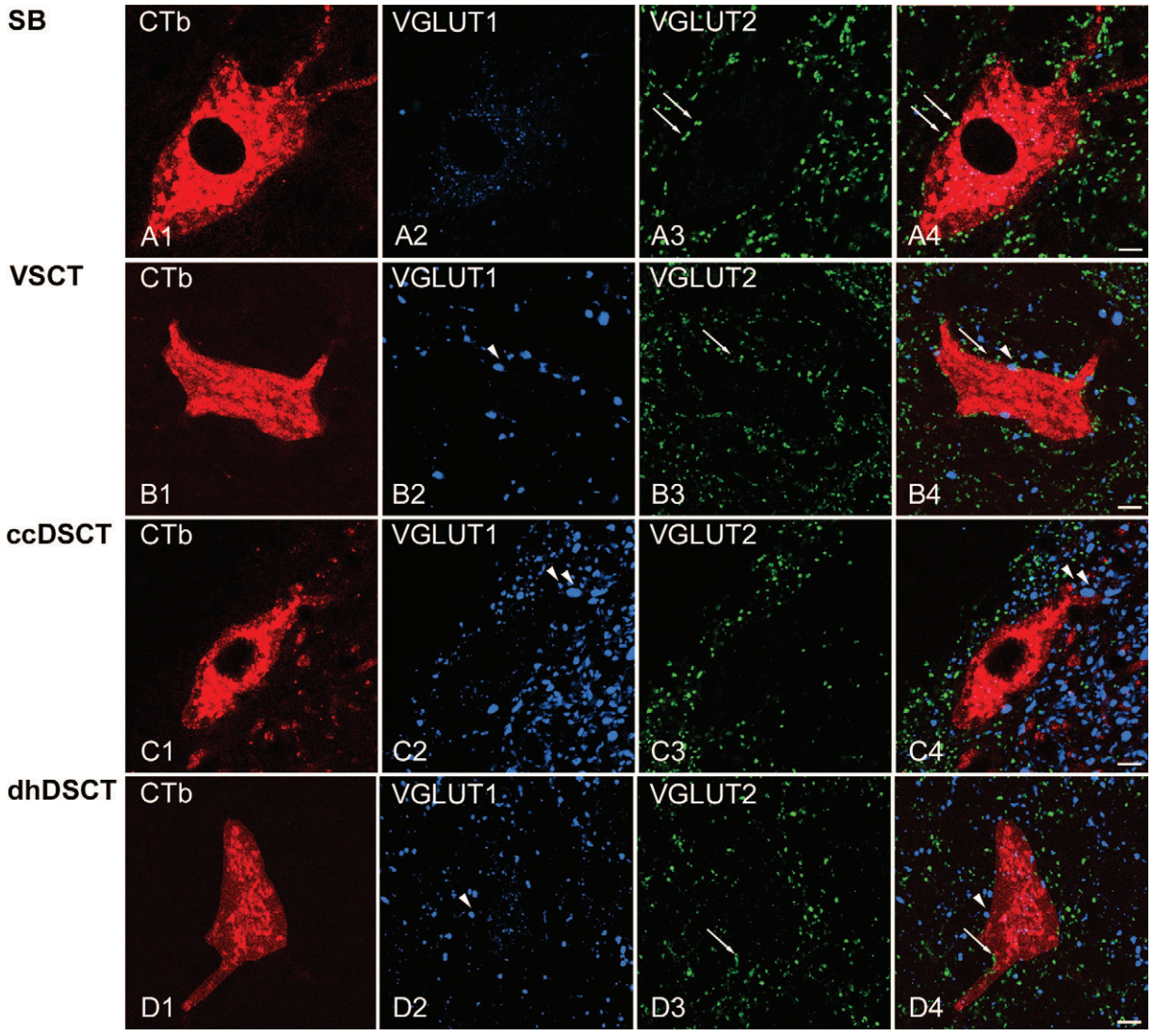

Figure 9. Immunohistochemical characteristics of VGLUT1 and VGLUT2 axon terminals in contact with retrogradely labelled spinocerebellar neurons
*A*1–*A*4, *B*1–*B*4, *C*1–*C*4 and *D*1–*D*4, single optical sections through the cell bodies of representative SB, VSCT, ccDSCT and dhDSCT neurons illustrating the contacts made by VGLUT1 (blue) and VGLUT2 (green) immunoreactive boutons indicated by arrowheads and arrows, respectively. The cell body and dendrites of retrogradely labelled cells are in red. Note differences in the density of VGLUT1- and VGLUT2-immunoreactive terminals within different regions of the grey matter shown in *A*–*D* and especially the high density of VGLUT1 and low density of VGLUT2 within Clarke's column shown in *C*. Scale bar in *A*–*D*, 10 μm.

0.16 ± 0.07 per $100\,\mu m^2$. This difference was highly significant (Student's t test, $P < 0.001$). In contrast, in dhDSCT neurons, the overall average contact density of VGLUT1 terminals was 0.21 ± 0.04 per $100\,\mu m^2$ and that of VGLUT2 was 0.36 ± 0.13 per $100\,\mu m^2$ of the neuron. This difference was also statistically significant (Student's t test, $P < 0.05$).

Comparison of the overall contact densities on ccDSCT and dhDSCT neurons revealed a strong statistically significant difference for VGLUT1 terminals ($P < 0.001$; ANOVA) whereas differences in the overall contact density of VGLUT2 terminals were not significant (cf. data for cat cells above).

Comparison of cat and rat contacts

Comparison of the coverage by VGLUT1 and VGLUT2 terminals of spinocerebellar tract neurons in the cat and in the rat in Fig. 5 and Table 2 & 3 reveals two main features. Firstly, the overall contact densities of VGLUT1- as well as VGLUT2-immunoreactive terminals were 3–4 times lower on rat neurons. Possible reasons for this difference are discussed below. Secondly, there is a similar pattern of relative contact densities between each class of neuron in both species (Fig. 5); i.e. from the lowest densities of VGLUT1 terminals on SB neurons to the highest densities on ccDSCT neurons and from the highest densities of VGLUT2 terminals on SB neurons to the lowest densities on ccDSCT neurons.

Discussion

The results of this study revealed significant differences in patterns of excitatory axonal contacts on four populations of spinocerebellar tract neurons in cats and rats.

It is well established that VGLUT1 and VGLUT2 are the transporters that are present in the axons of glutamatergic neurons within the spinal cord and that all myelinated primary afferent terminals in the grey matter of lumbar spinal cord, with the exception of those in lamina I, express VGLUT1 (Varoqui *et al.* 2002; Todd *et al.* 2003; Alvarez *et al.* 2004). Terminals of spinal interneurons and most glutamatergic descending tract neurons express VGLUT2; the exception to this is the corticospinal tract which contains VGLUT1 only (A. Du Beau, S. Shakya Shrestha and D. J. Maxwell, in preparation). Hence, the results of the present study substantiate the conclusion based on electrophysiological experiments (see Introduction) that SB neurons receive direct input mainly from intraspinal and supraspinal neurons. In contrast, negligible or weak input via VGLUT2-immunoreactive terminals to ccDSCT neurons in the cat makes it unlikely that these neurons receive major input from non-primary afferent excitatory neurons, with the possible exception of corticospinal neurons (Hantman & Jessell, 2010). Our results also indicate that differences in input from primary afferents and from other excitatory intraspinal and supraspinal neurons to VSCT and dhDSCT neurons are much less marked and therefore may have equally powerful actions on these cells.

Methodological issues

The numbers of spinocerebellar neurons of the four kinds on which the analysis is based in this study are small but we consider our samples of these neurons to be sufficiently representative because significant differences were found between each type while properties of neurons within them were reasonably consistent. The differences between the four types of spinocerebellar neurons were both qualitative and quantitative. Qualitative differences in the presence or absence and in the distribution of VGLUT1- and VGLUT2-positive terminals illustrated in Figs 4 and 6 are, in fact, so striking that they hardly require quantitative analysis to substantiate them. The comparison of numbers of VGLUT1- and VGLUT2-positive terminals on SB and VSCT neurons (cats, Table 2; rats, Table 3 and Fig. 5) accordingly showed very highly significant differences between them. Highly significant differences were also found between numbers of VGLUT1- or VGLUT2-positive terminals in contact with VSCT and DSCT neurons.

Criteria for classification on the basis of coupling between primary afferents and selected spinocerebellar neurons and according to anatomical location in the lumbar grey matter also require some comments. Properties of main populations of spinocerebellar neurons were previously outlined in electrophysiological and morphological studies in the cat. Using this knowledge we could therefore reliably classify individual neurons encountered during electrophysiological exploration of the spinal cord into one of these populations. In addition, we could select subpopulations within a given group, in particular a subpopulation of SB cells with dominant inhibitory input from peripheral afferents and monosynaptic input from reticulospinal tract neurons (Burke *et al.* 1971; Jankowska *et al.* 2010; Hammar *et al.* 2011) and subsequent verification of location and morphology of the labelled neurons fully confirmed original classifications.

The density of contacts on cat spinocerebellar tract cells was generally 3–4 times higher than that associated with rat cells. Whilst the reason for this difference is unclear at least part of the explanation is the incomplete labelling of dendritic arbors of retrogradely labelled cells. Sholl analysis of contacts on dendrites of cat neurons reveals that even the most distal parts of the dendrites are associated with substantial numbers of VGLUT1 and/or VGLUT2 terminals (see below). As the surface area of the dendrites is small, the mean values of contact densities

Table 3. The number and densities of VGLUT1 and VGLUT2 axon terminals in apposition with the cell bodies and dendrites of different populations of retrogradely labelled spinocerebellar tract neurons in rats

					Soma					Dendrite					
Populations of spinocerebellar tract neurons	Animal	No. of cells	Contacts (total number)		Contacts (*n*)		Surface area (μm^2)	Density (*n*/100 μm^2)		Contacts (*n*)		Total dendritic length (μm)	Surface area (μm^2)	Density (*n*/100 μm^2)	
			VGLUT1	VGLUT2	VGLUT1	VGLUT2		VGLUT1	VGLUT2	VGLUT1	VGLUT2			VGLUT1	VGLUT2
SB															
	Rat 1	3	2	126	1	20	6859.79	0.01	0.29	1	106	374.00	5050.97	0.02	2.10
	Rat 2	3	1	71	1	17	3766.96	0.03	0.45	0	54	107.70	2018.07	0.00	2.68
	Rat 3	7	2	125	1	36	7070.03	0.01	0.51	1	89	155.51	3769.65	0.03	2.36
	Rat 4	5	0	123	0	40	6755.2	0.00	0.59	0	83	136.24	3166.41	0.00	2.62
Mean								**0.01**	**0.46**					**0.01**	**2.44**
SD								**0.01**	**0.13**					**0.01**	**0.27**
VSCT															
	Rat 1	4	24	52	10	11	7015.04	0.14	0.16	14	41	260.63	6875.58	0.20	0.60
	Rat 2	4	8	39	2	5	5004.42	0.04	0.10	6	34	267.05	5277.05	0.11	0.64
	Rat 3	3	2	94	1	33	5448.27	0.02	0.61	1	61	130.17	2857.12	0.04	2.14
	Rat 4	6	6	112	2	23	4860.67	0.04	0.47	4	89	207.18	3987.45	0.10	2.23
Mean								**0.06**	**0.33**					**0.11**	**1.40**
SD								**0.06**	**0.24**					**0.07**	**0.90**
ccDSCT															
	Rat 1	5	39	6	12	2	4602.70	0.26	0.04	27	4	107.74	3436.65	0.79	0.12
	Rat 2	7	31	8	12	3	2740.30	0.44	0.11	19	5	118.94	1939.90	0.98	0.26
	Rat 3	5	40	10	17	4	3004.15	0.57	0.13	23	6	51.14	1186.31	1.94	0.51
	Rat 4	7	37	6	8	2	3341.03	0.24	0.06	29	4	85.89	1723.13	1.68	0.23
Mean								**0.38**	**0.09**					**1.35**	**0.28**
SD								**0.15**	**0.04**					**0.55**	**0.16**
dhDSCT															
	Rat 1	5	17	18	6	7	4208.02	0.14	0.17	11	11	172.58	4285.35	0.26	0.26
	Rat 2	7	6	10	1	2	1812.43	0.06	0.11	5	8	110.40	1498.88	0.33	0.53
	Rat 3	6	11	25	2	5	2504.78	0.08	0.20	9	20	127.80	2454.00	0.37	0.81
	Rat 4	3	4	15	1	4	2229.03	0.04	0.18	3	11	80.6	1816.72	0.17	0.61
Mean								**0.08**	**0.16**					**0.28**	**0.55**
SD								**0.04**	**0.04**					**0.09**	**0.23**

will therefore be higher in the cat. Contact densities on rat dendrites were found to be considerably lower than those associated with cat dendrites whereas contact densities on cell bodies of both species were similar (see Tables 2 and 3). Nevertheless differences have been also found in the densities of contacts on the soma; for example, rat dhDSCT somata had considerably lower densities for VGLUT1 and VGLUT2 when compared with their cat counterparts. It should be noted that cell bodies of all types of rat spinocerebellar tract neurons are smaller than those in the cat and therefore they may require less excitatory drive to activate them.

Origin and patterns of excitatory axonal contact on different populations of spinocerebellar neurons

SB and VSCT neurons. Our morphological analysis revealed that VSCT neurons have much higher numbers of contacts from VGLUT1-immunoreactive terminals than SB neurons in both cats and rats. They show also that there are no reasons to assume that SB neurons with dominating inhibitory input from low threshold afferent fibres in the main branches of the sciatic nerve might receive direct excitatory input from higher threshold afferents in the same nerves or from afferent fibres from other parts of the body (e.g. from the most distal or most proximal parts of the limbs or from trunk; see Introduction).

However, this conclusion may be valid only for a fraction of feline SB neurons located in the L3–L4 segments where only IPSPs can be evoked from stimulated muscle nerves (Burke *et al.* 1971; Jankowska *et al.* 2010; Hammar *et al.* 2011). As a higher proportion of more caudally located SB neurons were found to be monosynaptically excited by group I afferents (Burke *et al.* 1971), a greater density of VGLUT1-positive terminals would be predicted to be present on these neurons.

Differences in direct input from primary afferents are also relevant to the problem of subdivision of VSCT neurons into SB and more medially located subpopulations (see Introduction). The borderlines between these subpopulations are not very sharp, whether in terms of location or of synaptic input predominantly from group Ib or group Ia afferents, but the present results support this functional subdivision and are compatible with differential activation of VSCT and SB neurons and their proposed functions (see Lundberg, 1971; Hammar *et al.* 2011) as well as their differential projections to

the cerebellum (Matsushita & Ikeda, 1980; Matsushita & Hosoya, 1982; Matsushita & Yaginuma, 1989).

The number of VGLUT2 terminals in contact with VSCT and SB neurons likewise differed, both in the cat and in the rat, but the reasons for this difference are less clear. Previous electrophysiological studies revealed that both SB and VSCT neurons are sometimes di- and poly-synaptically excited from muscle, tendon organ and cutaneous afferents (Eccles *et al.* 1961*a*; Lundberg & Oscarsson, 1962; Lundberg, 1971) so that VGLUT2 terminals could originate from excitatory interneurons mediating indirect actions of peripheral afferents upon these neurons. However, descending tract fibres provide direct excitatory input to both SB and VSCT neurons (Baldissera & ten Bruggencate, 1976; Hammar *et al.* 2011) and could be another source of VGLUT2-immunoreactive terminals (Du Beau, S. Shakya Shrestha and D. J. Maxwell, in preparation). Excitatory interneurons contacting SB and VSCT neurons might include interneurons located in the intermediate zone with group I/II inputs and ipsilateral terminations outside motor nuclei in addition to those within motoneuron pools (Bannatyne *et al.* 2009). However, these interneurons are less likely to be involved in relaying indirect actions of reticulospinal neurons because the majority of contacts on them are made by VGLUT1-positive terminals and there are very few from VGLUT2 terminals, thus indicating that they receive inputs mainly from primary afferents (Liu *et al.* 2010). Indirect excitatory actions of reticulospinal neurons are more likely to be mediated by lamina VIII commissural interneurons projecting to areas outside motor nuclei, including medial and lateral lamina VII and VIII which are known to have VGLUT2-immunoreactive terminals (Jankowska *et al.* 2009).

Clarke's column and dorsal horn DSCT neurons. Electrophysiological and morphological studies have established that two functionally distinct populations of cells form components of the DSCT: ccDSCT and dhDSCT (for review see Bosco & Poppele, 2001), but that both receive strong monosynaptic input from primary afferents: ccDSCT neurons mainly from group I afferents (Eccles *et al.* 1961*b*) and dhDSCT neurons from group II and cutaneous afferents (Edgley & Jankowska, 1988). Some disynaptic excitatory actions were also postulated (Eccles *et al.* 1961*b*; Edgley & Jankowska, 1988; Krutki *et al.* 2011). However, the paucity of VGLUT2 contacts on ccDSCT neurons makes it unlikely that any major excitatory input is provided to them by interneurons in neuronal pathways that have not been explored in electrophysiological experiments. This conclusion is consistent with the observations of Krutki *et al.* (2011) who were able to evoke disynaptic EPSPs in dhDSCT cells but not in ccDSCT cells following stimulation applied within motor nuclei. Furthermore, the paucity of VGLUT2 contacts on ccDSCT neurons suggests that it is unlikely that they are involved to any major extent in processing information from supraspinal neurons with the exception of corticospinal neurons which constitute an additional source of input to ccDSCT neurons at least in mice (Hantman & Jessell, 2010).

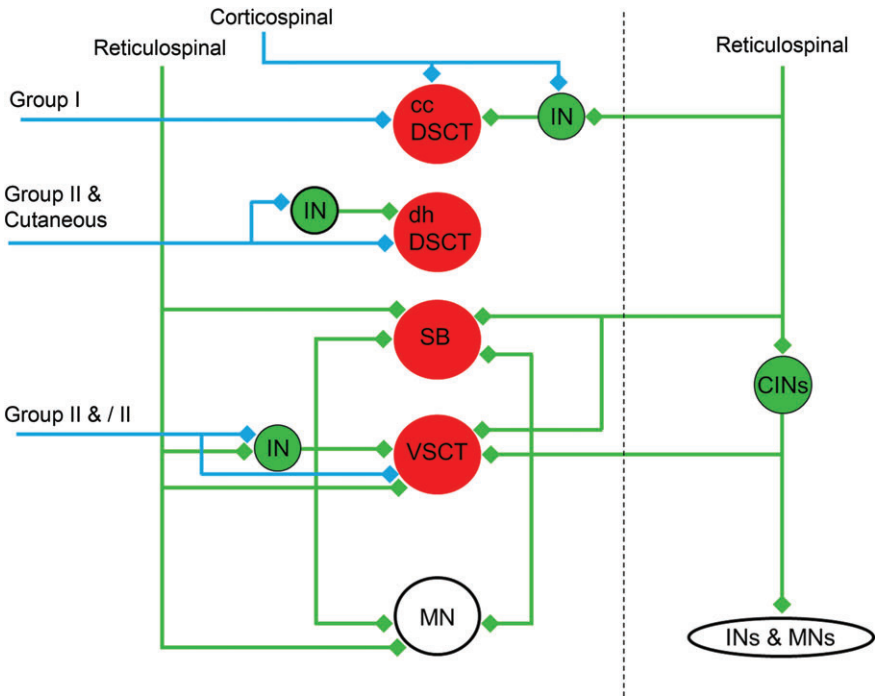

Figure 10. Putative excitatory contacts formed with the four different populations of lumbar spinocerebellar tract neurons
Red circles represent Clarke's column in dorsal spinocerebellar tract neurons (ccDSCT), dorsal horn dorsal spinocerebellar tract neurons (dhDSCT), spinal border neurons (SB) and Ib-ventral spinocerebellar tract neurons (VSCT). Green circles represent excitatory interneurons in reflex pathways to motoneurons (MN) activated by primary afferents and descending systems. Blue lines and diamonds represent neurons that express vesicular glutamate transporter 1 (VGLUT1) in their axon terminals. Green lines and diamonds represent neurons that express vesicular glutamate transporter 2 (VGLUT2) in their axon terminals. CINs, commissural interneurons; INs, interneurons; MNs, motoneurons.

Differential distribution of VGLUT1 and VGLUT2 contacts

Sholl analysis in the intracellularly labelled cat neurons shown in Fig. 6 reveals that VGLUT2 boutons are concentrated around proximal dendrites of SB and VSCT neurons whereas VGLUT1 contacts dominate on the proximal dendrites of DSCT neurons. There is limited information on distribution patterns of excitatory terminals associated with other spinal neurons. In a study by Liu *et al.* (2010) on intermediate zone interneurons, it was found that VGLUT1 terminals predominated on both inhibitory and excitatory cells and were most concentrated around proximal dendrites. Excitatory cells were almost devoid of VGLUT2 terminals whereas inhibitory cells had relatively low densities of VGLUT2 contacts that were evenly distributed through their dendritic trees. As a similar pattern of distribution was identified for VGLUT1 terminals in contact with DSCT cells, this may represent a pattern for primary afferent input. The consequences of the differential distribution of VGLUT1 and VGLUT2 contacts for the efficiency of synaptic actions evoked from different sources cannot be predicted until more is known about characteristics of the synaptic contacts and cable properties of dendrites of both ascending tract cells and interneurons in which such differences occur. However, one may expect different shape indices of excitatory post synaptic potentials (EPSPs) evoked at different distances from soma, including time to peak, half-width, as well as the latency and amplitude, and differences in the linearity of summation and final effects on the spike-generating region (Rall *et al.* 1967; Rall, 1977; Korogod & Tyc-Dumont, 2010).

Functional considerations

The present findings provide a new basis for understanding the organization and functional connectivity of four populations of spinocerebellar tract neurons in the lumbar enlargement of the cat and in thoraco-lumbar segments in the rat and strengthen previous indications of their functional differentiation. Putative excitatory connections of the four populations of neurons based on our findings combined with information from previous studies are summarized in Fig. 10.

The role of DSCT neurons is not limited to the integration of proprioceptive and extereoceptive sensory inputs. For instance, ccDSCT neurons also integrate cortical inputs (Hantman & Jessell, 2010) allowing predictions of the sensory consequences of motor acts from higher centres in anticipation of peripherally derived sensory feedback. However, very scarce input via VGLUT2-immunoreactive contacts in cats makes it unlikely that ccDSCT neurons are involved in relaying actions of intrinsic interneuronal networks. It is also unlikely that rhythmic locomotor-like activity reported in ccDSCT neurons (H. Hultborn, personal communication) can be attributed to actions of excitatory spinal networks. Our findings are in good agreement with the demonstration that VSCT neurons receive inputs from inhibitory premotor interneurons as well as sensory fibres and might therefore supply the cerebellum with information about activity in interneuronal pathways to motoneurons (Lundberg, 1971; Arshavsky *et al.* 1972, 1984). They also provide convincing evidence that SB neurons, in which no excitatory actions are found from peripheral nerves, do indeed lack direct input from peripheral afferents. However, the considerable density of VGLUT2-immunoreactive contacts on VSCT and SB neurons is not matched by the widespread but relatively weak supraspinal input to them. Some intraspinal sources of excitatory input to these neurons have been discussed above, but many more would be expected. Lack of peripheral excitatory input to SB neurons has led to the conclusion that they forward information on spinal actions of descending commands depending on the degree of inhibition of motoneurons (Hammar *et al.* 2011). However, even though the role of SB and VSCT neurons in monitoring actions of inhibitory premotor interneurons on motoneurons may be particularly important, excitatory inputs to these neurons mediated via yet undefined spinal neurons might likewise provide the cerebellum with important information.

References

Alvarez FJ, Villalba RM, Zerda R & Schneider SP (2004). Vesicular glutamate transporters in the spinal cord, with special reference to sensory primary afferent synapses. *J Comp Neurol* **472**, 257–280.

Arshavsky YI, Berkinblit MB, Fukson OI, Gelfand IM & Orlovsky GN (1972). Origin of modulation in neurones of the ventral spinocerebellar tract during locomotion. *Brain Res* **43**, 276–279.

Arshavsky YI, Gelfand IM, Orlovsky GN, Pavlova GA & Popova LB (1984). Origin of signals conveyed by the ventral spino-cerebellar tract and spino-reticulo-cerebellar pathway. *Exp Brain Res* **54**, 426–431.

Baldissera F & Roberts WJ (1976). Effects from the vestibulospinal tract on transmission from primary afferents to ventral spino-cerebellar tract neurones. *Acta Physiol Scand* **96**, 217–232.

Baldissera F & ten Bruggencate G (1976). Rubrospinal effects on ventral spinocerebellar tract neurones. *Acta Physiol Scand* **96**, 233–249.

Bannatyne BA, Liu TT, Hammar I, Stecina K, Jankowska E & Maxwell DJ (2009). Excitatory and inhibitory intermediate zone interneurons in pathways from feline group I and II afferents: differences in axonal projections and input. *J Physiol* **587**, 379–399.

Bosco G & Poppele RE (2001). Proprioception from a spinocerebellar perspective. *Physiol Rev* **81**, 539–568.

Burke R, Lundberg A & Weight F (1971). Spinal border cell origin of the ventral spinocerebellar tract. *Exp Brain Res* **12**, 283–294.

Drummond GB, Paterson DJ & McGrath JC (2010). ARRIVE: new guidelines for reporting animal research. *J Physiol* **588**, 2517.

Eccles JC, Hubbard JI & Oscarsson O (1961*a*). Intracellular recording from cells of the ventral spinocerebellar tract. *J Physiol* **158**, 486–516.

Eccles JC, Oscarsson O & Willis WD (1961*b*). Synaptic action of group I and II afferent fibres of muscle on the cells of the dorsal spinocerebellar tract. *J Physiol* **158**, 517–543.

Edgley SA & Jankowska E (1987). Field potentials generated by group II muscle afferents in the middle lumbar segments of the cat spinal cord. *J Physiol* **385**, 393–413.

Edgley SA & Jankowska E (1988). Information processed by dorsal horn spinocerebellar tract neurones in the cat. *J Physiol* **397**, 81–97.

Hammar I, Chojnicka B & Jankowska E (2002). Modulation of responses of feline ventral spinocerebellar tract neurons by monoamines. *J Comp Neurol* **443**, 298–309.

Hammar I, Krutki P, Drzymala-Celichowska H, Nilsson E & Jankowska E (2011). A trans-spinal loop between neurones in the reticular formation and in the cerebellum. *J Physiol* **589**, 653–665.

Hantman AW & Jessell TM (2010). Clarke's column neurons as the focus of a corticospinal corollary circuit. *Nat Neurosci* **13**, 1233–1239.

Jankowska E, Bannatyne BA, Stecina K, Hammar I, Cabaj A & Maxwell DJ (2009). Commissural interneurons with input from group I and II muscle afferents in feline lumbar segments: neurotransmitters, projections and target cells. *J Physiol* **587**, 401–418.

Jankowska E, Krutki P & Hammar I (2010). Collateral actions of premotor interneurons on ventral spinocerebellar tract neurons in the cat. *J Neurophysiol* **104**, 1872–1883.

Jankowska E, Nilsson E & Hammar I (2011). Processing information related to centrally initiated locomotor & voluntary movements by feline spinocerebellar neurones. *J Physiol* **589**, 5709–5725.

Korogod SM & Tyc-Dumont S (2010). *Electrical Dynamics of the Dendritic Space*. Cambridge University Press.

Krutki P, Jelen S & Jankowska E (2011). Do premotor interneurons act in parallel on spinal motoneurons and on dorsal horn spinocerebellar and spinocervical tract neurons in the cat? *J Neurophysiol* **105**, 1581–1593.

Liu TT, Bannatyne BA, Jankowska E & Maxwell DJ (2010). Properties of axon terminals contacting intermediate zone excitatory and inhibitory premotor interneurons with monosynaptic input from group I and II muscle afferents. *J Physiol* **588**, 4217–4233.

Lundberg A (1971). Function of the ventral spinocerebellar tract. A new hypothesis. *Exp Brain Res* **12**, 317–330.

Lundberg A & Oscarsson O (1962). Functional organization of the ventral spino-cerebellar tract in the cat. IV. Identification of units by antidromic activation from the cerebellar cortex. *Acta Physiol Scand* **54**, 252–269.

Lundberg A & Weight F (1971). Functional organization of connexions to the ventral spinocerebellar tract. *Exp Brain Res* **12**, 295–316.

Matsushita M & Hosoya Y (1979). Cells of origin of the spinocerebellar tract in the rat, studied with the method of retrograde transport of horseradish peroxidase. *Brain Res* **173**, 185–200.

Matsushita M & Hosoya Y (1982). Spinocerebellar projections to lobules III to V of the anterior lobe in the cat, as studied by retrograde transport of horseradish peroxidase. *J Comp Neurol* **208**, 127–143.

Matsushita M, Hosoya Y & Ikeda M (1979). Anatomical organization of the spinocerebellar system in the cat, as studied by retrograde transport of horseradish peroxidase. *J Comp Neurol* **184**, 81–106.

Matsushita M & Ikeda M (1980). Spinocerebellar projections to the vermis of the posterior lobe and the paramedian lobule in the cat, as studied by retrograde transport of horseradish peroxidase. *J Comp Neurol* **192**, 143–162.

Matsushita M & Yaginuma H (1989). Spinocerebellar projections from spinal border cells in the cat as studied by anterograde transport of wheat germ agglutinin-horseradish peroxidase. *J Comp Neurol* **288**, 19–38.

Oscarsson O (1965). Functional organization of the spino- and cuneocerebellar tracts. *Physiol Rev* **45**, 495–522.

Paxinos G. & Watson C (1997). The rat brain in stereotaxic coordinates. 3rd. 2003. New York, Academic Press.

Rall W (1977). Core conductor theory and cable properties of neurons. In *The Nervous System*, ed. Kandel ER, pp. 39–97. American Physiological Society, Washington.

Rall W, Burke RE, Smith TG, Nelson PG & Frank K (1967). Dendritic location of synapses and possible mechanisms for the monosynaptic EPSP in motoneurons. *J Neurophysiol* **30**, 1169–1193.

Todd AJ, Hughes DI, Polgar E, Nagy GG, Mackie M, Ottersen OP & Maxwell DJ (2003). The expression of vesicular glutamate transporters VGLUT1 and VGLUT2 in neurochemically defined axonal populations in the rat spinal cord with emphasis on the dorsal horn. *Eur J Neurosci* **17**, 13–27.

Varoqui H, Schafer MK, Zhu H, Weihe E & Erickson JD (2002). Identification of the differentiation-associated Na^+/PI transporter as a novel vesicular glutamate transporter expressed in a distinct set of glutamatergic synapses. *J Neurosci* **22**, 142–155.

Author contributions

All authors were involved in designing the study. S.S.S., B.A.B. and D.J.M. analysed the immunocytochemistry of glutamatergic terminals. E.J., I.H. and E.N. performed the electrophysiological experiments in which the spinocerebellar neurons were selected, identified and labelled. S.S.S. wrote the paper and prepared the illustrations, D.J.M. and E.J. contributed to its editing. All authors approved the final version.

Acknowledgements

This work was supported by a grant from NINDS/NIH. S.S.S. is supported by a University of Glasgow postgraduate scholarship and the Scottish Overseas Research Student Awards Scheme (SORSAS). B.A.B. was supported by the Wellcome Trust. We are grateful to Robert Kerr, Christine Watt and Jytte Grännsjö for excellent technical support. The authors are not aware of any conflict of interest.